

VARIATIONAL MONTE CARLO STUDY OF TWO DIMENSIONAL CHARGED BOSONS

A THESIS

SUBMITTED TO THE DEPARTMENT OF PHYSICS
AND THE GRADUATE SCHOOL OF ENGINEERING AND SCIENCE
OF BILKENT UNIVERSITY
IN PARTIAL FULFILLMENT OF THE REQUIREMENTS
FOR THE DEGREE OF
MASTER OF SCIENCE

By

Seher Karakuzu

September, 2014

I certify that I have read this thesis and that in my opinion it is fully adequate, in scope and in quality, as a thesis for the degree of Master of Science.

Assist. Prof. Dr. Balazs Hetényi(Advisor)

I certify that I have read this thesis and that in my opinion it is fully adequate, in scope and in quality, as a thesis for the degree of Master of Science.

Prof. Dr. Bilal Tanatar

I certify that I have read this thesis and that in my opinion it is fully adequate, in scope and in quality, as a thesis for the degree of Master of Science.

Assoc. Prof. Dr. Azer Kerimov

Approved for the Graduate School of Engineering and Science:

Prof. Dr. Levent Onural
Director of the Graduate School

ABSTRACT

VARIATIONAL MONTE CARLO STUDY OF TWO DIMENSIONAL CHARGED BOSONS

Seher Karakuzu

M.S. in Physics

Supervisor: Assist. Prof. Dr. Balazs Hetényi

September, 2014

We studied the ground state properties of 2D charged Bosons interacting via Coulomb potential using the Variational Monte Carlo method. We start with the paper of McMillan [1] in which there are 3D Bosons interacting via Lennard-Jones potential. We calculate ground state energy and pair distribution function of the system and our results are compared with the original work. We also reproduce the paper of Liu et al. [2] and study the 2D Bosons interacting with the same potential. Our results are compared with the original work. In order to evaluate long-range potentials in periodic systems we introduce Ewald summation method for 2D system and Natoli-Ceperley method which evaluates potentials optimally. We compare our Natoli-Ceperley results with the Holzmann et al. [3]. We also investigate 2D charged Boson system interacting via Coulomb potential using the RPA pseudo potential. Our results are compared with de Palo et al. [4]. We try to optimize the wave function further introducing a Kinetic Energy projection to the original RPA wave function. We show that it is very difficult to optimize it further since it is a very good wave function.

Keywords: Electron gas, Bose gas, Variational Monte Carlo, RPA, Ewald Summation, Natoli-Ceperley.

ÖZET

İKİ BOYUTTAKİ YÜKLÜ BOZONLARIN VARYASYONEL MONTE CARLO ÇALIŞMASI

Seher Karakuzu

Fizik, Yüksek Lisans

Tez Yöneticisi: Yard. Doç. Dr. Balazs Hetényi

Eylül, 2014

Varyasyonel Monte Carlo metodunu kullanarak iki boyutta Coulomb potansiyeli ile etkileşen yüklü Bozonların taban seviye özelliklerini çalıştık. üç boyutta Lennard-Jones potansiyeli ile etkileşen Bozonların çalışıldığı McMillan'ın makalesi [1] ile başladık. Sistemin taban seviyesi enerjisini ve ikili dağılım fonksiyonunu hesaplayıp sonuçlarımızı orijinal makale ile karşılaştırdık. Liu ve arkadaşlarının [2] aynı potansiyelle etkileşen iki boyutta Bozon parçacıklarını çalıştıkları makaleye geçtik. Sonuçlarımızı orijinal makale ile karşılaştırdık. Periyodik sistemlerde uzun menzilli potansiyellerin hesaplanması için Ewald Toplama metodunu ve Natoli-Ceperley metodunu tanıttık. Sonuçlarımızı Holzmann ve arkadaşlarının makalesi [3] ile karşılaştırdık. İki boyutta Coulomb potansiyeli ile etkileşen ve RPA sahte potansiyeli ile bağlantı kuran Bozon sistemine geçtik. Sonuçlarımızı de Palo ve arkadaşlarının [4] sonuçları ile karşılaştırdık. Orijinal RPA dalga fonksiyonuna Kinetik projeksiyon tanıtarak dalga fonksiyonunu daha da iyileştirmeye çalıştık. Dalga fonksiyonunun çok iyi olmasından dolayı daha da iyileştiremeyeceğimizi gösterdik.

Anahtar sözcükler: Elektron gazı, Bozon gazı, Varyasyonel Monte Carlo, RPA, Ewald Toplaması, Natoli-Ceperley.

Acknowledgement

I would like to thank my advisor Assist. Prof. Dr. Balazs Hetényi for his support, guidance and for the time he spent for me during the semester.

I would like to give many thanks to Prof. Bilal Tanatar for his encouragement, valuable guidance and friendly attitude. I am grateful for having had the chance to study under his supervision and to have his academic and personal advice.

I would like to thank Assoc. Prof. Dr. Azer Kerimov for taking the time to read my thesis and for his valuable feedback.

Also, I am grateful to have the chance to thank TÜBİTAK-BİDEB for their financial support during my B.S. and M.S. studies.

Contents

1	Introduction	1
1.1	Outline of the Thesis	2
2	Monte Carlo Methods	3
2.1	Markov chains and the Metropolis Algorithm	5
2.2	Variational Monte Carlo	7
2.2.1	VMC Study of 3 Dimensional Liquid He4	9
2.2.2	VMC Study of 2 Dimensional Liquid He4	13
3	Ewald Summation and Natoli-Ceperley Method	16
3.1	Ewald Sum	17
3.2	Natoli-Ceperley Method	18
3.2.1	LPQHI	21
3.2.2	Two Dimensional Optimized Coulomb	23
4	Two Dimensional Charged Bose Gas	26

4.1	Electron Gas	26
4.2	Bose Gas	28
5	Projected Wave Functions	33
5.1	Kinetic Energy Projection of RPA Wave Function	33
6	Conclusion	39

List of Figures

2.1	The energy diagram for the 3 dimensional liquid Helium4 for different values of a_1 and a_2	12
2.2	The pair distribution function for the 3 dimensional liquid Helium4 for the variational parameter $a_1=2.6$ and $a_2=5$	13
2.3	The energy plot for the 2 dimensional liquid Helium4 for $b=1.2$. .	14
2.4	The pair distribution function of the 2 dimensional liquid Helium4 for the density values of $\rho\sigma^2=0.4$ and for $\rho\sigma^2= 0.234$ for $b=1.2$. .	14
3.1	The LPQHI (locally piecewise quintic Hermite interpolants) and its derivatives	22
3.2	The difference between the optimized potential of ours and the one of Holzmann et al. :Red one is the difference between the potentials through the corner of the box and green one is the difference through the middle of the box length	24
4.1	The pair distribution function of 2D charged boson system for $r_s=1,2,5,10,20,40,75$	30
4.2	The energy plot VMC,DMC results for $r_s^{3/2} * (E(r_s) - c_1/r_s)$ where $c_1=-2.2122$ is the madelung constant for 2D lattice	31

4.3	The energy plot VMC,DMC results and for the WC calculations by Rapisarda et al. for $r_s^{3/2} * (E(r_s) - c_1/r_s)$ where $c_1=-2.2122$ is the madelung constant for 2D lattice	32
5.1	The energy values of 2D boson system with a projected wave function for different values of projection coefficient α for the density $r_s=5$	36
5.2	The energy values of 2D boson system with a projected wave function for different values of projection coefficient α for the density $r_s=20$	37
5.3	The energy values of 2D boson system with a projected wave function for different values of projection coefficient α for the density $r_s=40$	37
5.4	The energy values of 2D boson system with a projected wave function for different values of projection coefficient α for the density $r_s=75$	38

List of Tables

2.1	The Kinetic, Potential and Total energy values in units of ergs/atom for different values of the variational parameter a_1 and a_2	11
3.1	Our results and results from Holzmann et al. for y_k values for $N_{spline} = 2$ and $K_c = 4\pi/L$	24
4.1	VMC calculations of potential, kinetic and total energies of the 2D charged bosons for different number of particles and the extrapolated energy results (E_∞) with their standard deviations.	29
4.2	Energy results of de Palo et al for VMC, DMC calculations, our VMC calculations, STLS, STW and HNC calculations	30

Chapter 1

Introduction

The Electron Gas also called One Component Plasma is one of the most interesting models of electronic systems. Many theories have been developed in order to understand the properties of Electron Gas. Hartree-Fock theory formulated by Hartree and Fock is one of the first theories of all. Hartree-Fock theory approximates the wave function of electron system as a Slater determinant composed of one particle wave functions [5]. This type of wave function also accounts for the antisymmetry when exchange between electrons occurs. However, due to the long-range behaviour of the Coulomb potential some physical properties of the system, like specific heat, diverge when treated by perturbative approaches. In 1952 Bohm and Pines introduced the Random Phase Approximation (RPA) method to describe collective excitations of the electron gas [6, 7]. In 1961 Gaskell derived an optimized wave function composed of Slater determinants and an optimized Jastrow correlation function using the RPA method [8, 9]. Using the optimal form of the pseudo potential Ceperley calculated the energy, pair distribution functions of 2D and 3D electron gas using Variational Monte Carlo (VMC) method [10]. In 1989 Tanatar and Ceperley calculated the ground state properties of 2D electron gas using fixed-node Green's function Monte Carlo [11].

The charged boson system was not very attractive for condensed matter physicist since there is no physical analog for such systems. Those systems are mainly applicable for subatomic and astronomic systems such as charged weak bosons

in subatomic physics [12], boson stars [13]. However, after the discovery of superconductivity charged bosons started to attract condensed matter scientists also, since such systems might provide explanation for it [14]. Foldy made calculations to investigate the physical properties of charged boson systems using Bogoliubov Approximation [15]. Some other analytical approaches such as HNC (hypernetted-chain approximation) calculations by Apaja et al. [16], STLS calculations by Gold [17] and STW calculations by Sim,Tao,Wu [18] have been developed. One of the first QMC calculations of charged bosons were done by Magro and Ceperley in 1994 [19] in order to investigate the superfluidity phase. They performed DMC and VMC calculations for 2D charged Bose system interacting via $\ln(r)$ potential and observed a phase transition from liquid to Wigner Crystal (WC) at $r_s=12$. Some other DMC calculation were done in order to investigate the physical properties such as energy, structure factor, momentum distribution of charged Bosons interacting via Coulomb potential in 2D and 3D [4, 20] using optimized RPA pseudo potential.

1.1 Outline of the Thesis

In Chapter 2 we will explain the main ideas of Monte Carlo (MC) Method and introduce Variational Monte Carlo (VMC) method. In order to check the correctness of our code we will reproduce the work of McMillan [1] which is one of the first examples of VMC method. Since we will study 2D we will also check our code for 2D system by reproducing the work of Liu et al. [2]. In Chapter 3 we will study long-range potential in finite systems and we will explain Ewald Summation. Also we will introduce Natoli-Ceperley method for evaluating long-range potentials and then we will reproduce the work of Holzmann et al. [3] which is 2D version of the method. In Chapter 4 we will talk about electron gas and introduce the optimized long-range pseudo potential derived by Gaskell [8, 9] and then pass to 2D Boson system studied by de Palo et al. [4]. After reproducing the work of de Palo et al. in Chapter 5 we will try to optimize the variational energies more by introducing a kinetic projection to the optimized wave function. In the Chapter 6 we will conclude our work.

Chapter 2

Monte Carlo Methods

Computer simulations are one of the most efficient ways to investigate the physical properties of many body systems. As the number of particles increase the total number of degrees of freedom increases as $3N$ in 3D with N particles, it is impossible to deal with that many variables analytically. Methods such as mean field theory or perturbative approaches are not sufficient to obtain reasonable predictions for the physical properties or phase transitions of the systems. For example, mean field theory for Ising model is not able to capture the true behaviour of the model in 1D. And also mean field theory does not take the correlations between the particles into account in order to simplify the complicated analytical expressions. Computational power started to be used during the Second World War for the production of nuclear weapons and for the simulations of physical systems. The first scientific simulations were done by Metropolis et al. in 1952 on the computer MANIAC to simulate a liquid [21, 22]. The algorithm they used was named as Metropolis algorithm which is the fundamental algorithm in Monte Carlo simulations.

Monte Carlo Methods are widely used in many areas of science and engineering such as physics, chemistry, medicine, economy. The Monte Carlo method performs multidimensional integration by stochastic process. One famous example of MC integration is the calculation of the number π by integrating the area of a unit circle by generating random numbers x and y and summing over

the states when $x^2 + y^2 \leq 1$. One of the most important advantage of MC integration is that one can evaluate multidimensional integration with less cost of computation time compared to famous numerical quadrature techniques such as Simpson's rule. There one divides the space of integration into mesh points and by using quadratic polynomials interpolate the adjacent points on which the values of the function are calculated and finally sum the areas between each adjacent mesh points [22]. This advantage is more realizable when the integration is done on a many body system which has N large number of particles so there are ND dimensions to be integrated. In addition to this advantage, most of the times the functions to be integrated such as the ones including Boltzmann factor have non negligible values in the very small interval of the integration region. Therefore, if one wants to integrate such kind of a function by using numerical quadrature one needs many mesh points to capture that region and integrate efficiently through that rapid change in the value of the function. However, as the number of mesh points M increase the number of integration points increases as M^{ND} so the needed integration time is too much [22]. MC methods are able to solve the problem of integration of the functions which are peaked at some area of integration and negligible anywhere else by sampling the distribution rather than representing it on a grid so that while integration most of the time is spent in places where the function contributes to the integral. This improvement is called importance sampling and widely used in large simulations [22]. In the Metropolis algorithm Markov chains are used to sample the equilibrium state which is defined by a probability distribution function and explained in detailed in the next section.

There are several kinds of Monte Carlo methods such as Variational Monte Carlo (VMC), Diffusion Monte Carlo (DMC), Path Integral Monte Carlo (PIMC). In this thesis the work was done by using VMC method.

2.1 Markov chains and the Metropolis Algorithm

Markov chain is a stochastic process in which a random configuration is evolved from another random one in an indeterministic way. Markov chains in MC simulations can be generated by using the pseudo random generator in the computer. For example, the new position of a particle in a Markov chain is a function of its old position and a random number so that the current position of the particle depends on just the one before not on the whole history of the system. In Monte Carlo simulations the aim is to sample the equilibrium distribution by using finite but large number of Markov chains. There are some properties of Markov chains which lead to the equilibrium state. One of them is ergodicity that is in equilibrium any state must be reached from any other one in finite number of steps. The second one is the detailed balance condition.

For a system the probability current at a state is defined as the difference between the move of this state to the other ones and the moves done by other states to that state. In the equilibrium state the probability current is zero so a system's probability of moving from the state i to another state j is equal to the probability of moving from the state j to the state i [23].

$$\sum_j P(i)w(i \rightarrow j) = \sum_j P(j)w(j \rightarrow i) \quad (2.1)$$

where $P(i)$ is the probability for the particle to be in the state i and $w(i \rightarrow j)$ is the transition probability from state i to j . With the normalization property of the transition probability

$$\sum_j w(i \rightarrow j) = 1 \quad (2.2)$$

we have

$$P(i) = \sum_j P(j)w(j \rightarrow i) \quad (2.3)$$

To guarantee the equilibrium state in each Markov chain we apply detailed balance condition namely

$$P(i)w(i \rightarrow j) = P(j)w(j \rightarrow i) \quad (2.4)$$

In the paper of Metropolis et al. (1952) the transition probability is assumed to be the multiplication of probability of proposing the move and probability of accepting that move so that

$$P(i)T(i \rightarrow j)A(i \rightarrow j) = P(j)T(j \rightarrow i)A(j \rightarrow i) \quad (2.5)$$

if the matrix indicating the proposal of the move (T) is symmetric we get the original Metropolis algorithm (1952). Therefore, the ratio of the acceptance probabilities of a particles move is formulated as

$$\frac{A(i \rightarrow j)}{A(j \rightarrow i)} = \frac{P(j)}{P(i)} \quad (2.6)$$

Metropolis algorithm in MC simulations can be written in steps as below.

- Generate a configuration x_i
- Calculate the probability of the system being in that configuration, $P(x_i)$
- Generate another configuration x_{i+1} from x_i by Markovian process
- Calculate the probability of system being in state x_{i+1} , $P(x_{i+1})$
- Compare the probabilities of the two configuration and accept or reject the new configuration according to $A(x_i \rightarrow x_{i+1}) = \min\{1, \frac{P(x_{i+1})}{P(x_i)}\}$

If the move is accepted the new configuration is changed to x_{i+1} from x_i , otherwise the old configuration is kept. The Metropolis method weights the states by the probability distribution function $P(i)$ and calculates the average values of observables.

In classical statistical mechanics the probability distribution of a system is described by Boltzmann Distribution which is

$$P_i = \exp(-\beta E_i)/Z \text{ for } Z = \sum_i \exp(-\beta E_i) \quad (2.7)$$

where Z is the partition function, β is $1/k_B T$ for k_B is Boltzmann constant and E_i is the energy of i th state. The average value of any observable in the system can be calculated as

$$\langle A \rangle = \sum_i^M P_i A_i \quad (2.8)$$

where A_i is the value of the operator in i th state and M is the number states on which the measurement is performed. In the Monte Carlo approach of classical systems the samples are drawn from the Boltzmann distribution. Therefore the expectation values of observables can be calculated as

$$\langle A \rangle = \frac{1}{M} \sum_i^M A_i \quad (2.9)$$

Since in Metropolis algorithm we look only for the ratio of the energy of the states, we do not need to calculate the partition function. For example, as a classical system, the observables in Ising Model such as susceptibility, heat capacity can be calculated by applying random spin flips and the Metropolis algorithm above and very reliable results are obtained for phase transitions.

2.2 Variational Monte Carlo

In Quantum mechanics the expectation value of an operator \hat{A} can be expressed as

$$\langle \hat{A} \rangle = \frac{\int d\mathbf{R} \psi^*(\mathbf{R}) \hat{A} \psi(\mathbf{R})}{\int d\mathbf{R} \psi^*(\mathbf{R}) \psi(\mathbf{R})} \quad (2.10)$$

where ψ is the wave function of the system. Assuming that the $\psi(\mathbf{R})$ is a noddles function the equation can be re-expressed as below

$$\langle \hat{A} \rangle = \frac{\int d\mathbf{R} \psi^*(\mathbf{R}) \frac{\psi(\mathbf{R})}{\psi(\mathbf{R})} \hat{A} \psi(\mathbf{R})}{\int d\mathbf{R} \psi^*(\mathbf{R}) \psi(\mathbf{R})} \quad (2.11)$$

or as

$$\langle \hat{A} \rangle = \frac{\int d\mathbf{R} |\psi(\mathbf{R})|^2 \frac{1}{\psi(\mathbf{R})} \hat{A} \psi(\mathbf{R})}{\int d\mathbf{R} |\psi(\mathbf{R})|^2} \quad (2.12)$$

We can use the Metropolis integration scheme also for quantum systems since the probability distribution function can be defined as

$$P(\mathbf{R}) = \frac{|\psi(\mathbf{R})|^2}{\int d\mathbf{R} |\psi(\mathbf{R})|^2} \quad (2.13)$$

therefore with the samples chosen according to the probability distribution above the expectation value of the operator can be calculated as

$$\langle \hat{A} \rangle = \frac{1}{M} \sum_{i=1}^M \frac{1}{\psi(\mathbf{R}_i)} \hat{A} \psi(\mathbf{R}_i) \quad (2.14)$$

Wave functions describing the properties of the quantum systems may not be known exactly since many body quantum systems are very hard to deal with so one way that physicists use to approach the true behaviour of the system is to approximate the wave function. This method is called as variational method in quantum mechanics. A trial wave function is assumed to depend on some variational parameters and it establishes an upper bound for the ground state of the system. Therefore, any trial wave function ψ_T with some variational parameter α should obey the condition

$$\frac{\langle \psi_T(\alpha, \mathbf{R}) | \hat{H} | \psi_T(\alpha, \mathbf{R}) \rangle}{\langle \psi_T(\alpha, \mathbf{R}) | \psi_T(\alpha, \mathbf{R}) \rangle} \geq \varepsilon_0 \quad (2.15)$$

where ε_0 is the exact energy of the ground state of the system of interest. In the VMC calculations the energy values for any α is calculated and the most reasonable wave function for the system is defined as the one which produces lowest energy.

In the thesis some work has been done by using variational wave functions described in the papers of McMillan [1] and Liu et al. [2] in order to check the correctness of the code. The details of the calculations are explained in the upcoming sections.

2.2.1 VMC Study of 3 Dimensional Liquid He4

One of the first illustration of VMC for quantum systems is done by McMillan in 1965 [1] in order to investigate the ground state properties of He4 liquid. Hamiltonian for He4 liquid can be written as below

$$H = -\frac{\hbar^2}{2m} \sum_{i=1}^N \nabla_i^2 + \sum_{i<j=1}^N V(r_{ij}) \quad (2.16)$$

where i, j are particle subscripts and $V(r_{ij})$ is the two body potential. The particle interactions are assumed to be in the form of Lennard-Jones potential which is a smooth short ranged potential estimating the attractiveness and repulsiveness of particle at short and long distances.

$$V(r) = 4\epsilon \left[\left(\frac{\sigma}{r} \right)^{12} - \left(\frac{\sigma}{r} \right)^6 \right] \quad (2.17)$$

where $\epsilon = 10.22K^\circ$ and $\sigma = 2.556A^\circ$.

McMillan proposed a wave function of the form [1]

$$\psi = \prod_{i<j=1}^N f(r_{ij}) \quad (2.18)$$

where $f(r_{ij})$ is formulated as

$$f(r) = \exp\left[-\left(\frac{a_1}{r}\right)^{a_2}\right] \quad (2.19)$$

where a_1 and a_2 are variational parameters to be scanned in VMC calculations. In order to calculate the kinetic energy of the system we should take the second derivative of the wave function. Therefore, the second part of the Hamiltonian can be written as follows

$$\int \psi \nabla_i^2 \psi d\tau = \int \psi^2 \sum_{i \neq j} \nabla_i^2 \ln f(r_{ij}) d\tau + \int \psi \sum_{i \neq j} \nabla \ln f(r_{ij}) \cdot \nabla \psi d\tau \quad (2.20)$$

After integration by parts the expectation value of the Hamiltonian operator in other words the total energy of the system can be represented as below

$$\int \psi H \psi d\tau = \int \sum_{i < j} \left[\frac{-\hbar^2}{2m} \nabla_i^2 \ln f(r_{ij}) + V(r_{ij}) \right] \psi^2 d\tau \quad (2.21)$$

In the paper of McMillan [1] the energy of the liquid system with 32 particles forming an fcc lattice as a starting configuration is calculated and with an appropriate fit the energy of the ground state was found as $-0.77 \pm 0.09 \times 10^{-15}$ ergs/atom with the Angstrom (A°) is the unit of the length. McMillan used fcc configuration in the beginning of the simulation but the starting configuration does not matter since we are working with a liquid system so we calculated the ground state energy of the system by using 216 particles forming a square configuration at the beginning. The reason we used that many atoms is that we observed number dependence for small systems. We calculated the energy values for a_1 ranging from 2.1 to 3.2 and for a_2 is 4,5,6,8,10. The energies of a system with 216 particles and with the variational parameters explained above are tabulated in table 2.1

The energy plot in Fig.1 for each a_1 and a_2 values are drawn below in the range of the Fig.1 of the paper of McMillan. We obtain the ground state wave function, equation 2.15, for $a_1 = 2.6$ and for $a_2=5$ and the ground state energy of the 3 Dimensional Helium4 liquid as $-0.792921 \pm 0.276605 \times 10^{-15}$ ergs/atom

Table 2.1: The Kinetic, Potential and Total energy values in units of ergs/atom for different values of the variational parameter a_1 and a_2

a_1		$a_2=4$	$a_2=5$	$a_2=6$	$a_2=8$	$a_2=10$
2.1	$\langle K \rangle$	0.927035	1.10632	1.27046	1.59165	1.89979
	$\langle V \rangle$	4.3788	1.71062	0.542396	-0.317357	-0.607948
	$\langle E \rangle$	5.30584	2.81695	1.81285	1.2743	1.29184
2.2	$\langle K \rangle$	1.03148	1.23674	1.42544	1.781	2.12594
	$\langle V \rangle$	1.90886	-0.12871	-0.961976	-1.64045	-1.87804
	$\langle E \rangle$	2.94035	1.10803	0.463467	0.140556	0.247904
2.3	$\langle K \rangle$	1.14367	1.38372	1.60151	2.00047	2.38759
	$\langle V \rangle$	0.199825	-1.26923	-1.88624	-2.40658	-2.59761
	$\langle E \rangle$	1.3435	0.114494	-0.284729	-0.406109	-0.210019
2.4	$\langle K \rangle$	1.27035	1.5497	1.80187	2.26032	2.6946
	$\langle V \rangle$	-0.875927	-1.98964	-2.45074	-2.83706	-2.99009
	$\langle E \rangle$	0.394424	-0.439937	-0.648868	-0.576744	-0.295491
2.5	$\langle K \rangle$	1.40848	1.73603	2.02902	2.56313	3.05815
	$\langle V \rangle$	-1.61909	-2.45016	-2.79245	-3.06804	-3.18475
	$\langle E \rangle$	-0.210611	-0.714133	-0.763425	-0.504908	-0.126599
2.6	$\langle K \rangle$	1.56036	1.94563	2.29313	2.91582	3.48347
	$\langle V \rangle$	-2.11765	-2.73855	-2.98748	-3.18129	-3.26505
	$\langle E \rangle$	-0.557294	-0.792921	-0.694347	-0.265471	0.218419
2.7	$\langle K \rangle$	1.72659	2.1806	2.59028	3.33048	3.99563
	$\langle V \rangle$	-2.46007	-2.91834	-3.09267	-3.2223	-3.27643
	$\langle E \rangle$	-0.733477	-0.737735	-0.502395	0.108186	0.7192
2.8	$\langle K \rangle$	1.90862	2.44299	2.93593	3.81698	4.60805
	$\langle V \rangle$	-2.68931	-3.02511	-3.14217	-3.21966	-3.25018
	$\langle E \rangle$	-0.780694	-0.582116	-0.206234	0.597322	1.35788
2.9	$\langle K \rangle$	2.10774	2.73637	3.32592	4.39351	5.34399
	$\langle V \rangle$	-2.83986	-3.08421	-3.15697	-3.19258	-3.2033
	$\langle E \rangle$	-0.73212	-0.347844	0.168952	1.20094	2.14069
3.0	$\langle K \rangle$	2.32399	3.06442	3.77151	5.07282	6.23875
	$\langle V \rangle$	-2.94308	-3.11062	-3.14881	-3.15254	-3.14644
	$\langle E \rangle$	-0.61909	-0.0462043	0.6227	1.92029	3.09231
3.1	$\langle K \rangle$	2.55915	3.43027	4.2781	5.87382	7.31689
	$\langle V \rangle$	-3.00691	-3.11699	-3.12886	-3.10613	-3.08619
	$\langle E \rangle$	-0.447763	0.313279	1.14924	2.76769	4.2307
3.2	$\langle K \rangle$	2.81609	3.83576	4.85551	6.8196	8.6279
	$\langle V \rangle$	-3.04478	-3.11022	-3.10081	-3.05789	-3.02689
	$\langle E \rangle$	-0.228685	0.725543	1.7547	3.76172	5.60101

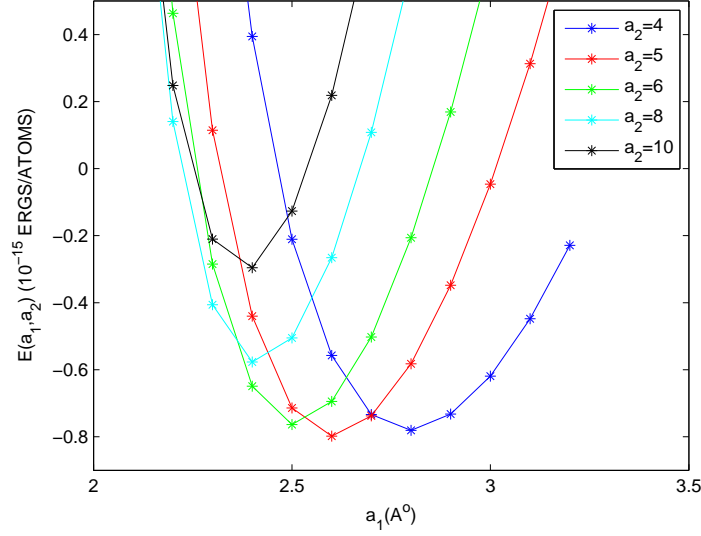


Figure 2.1: The energy diagram for the 3 dimensional liquid Helium4 for different values of a_1 and a_2

where the experimental ground state energy is -0.988×10^{-15} ergs/atom [1]. We obtained good agreement with the paper of McMillan in which the ground state wave function was found for values of $a_1 = 2.6$ and for $a_2=5$ and the energy of the system was found as $-0.77 \pm 0.09 \times 10^{-15}$ ergs/atom.

The pair distribution function represents the probability of any two particles to be in a particular distance from each other. The formulation can be written as follows

$$g(\mathbf{R}_1 - \mathbf{R}_2) = \frac{\frac{1}{\rho^2} \int \sum_{i \neq j} \delta(\mathbf{R}_1 - \mathbf{r}_i) \times \delta(\mathbf{R}_2 - \mathbf{r}_j) \psi^2 t \tau}{\int \psi^2 d\tau} \quad (2.22)$$

If the center of the box is origin, the pair distribution function is calculated for the half of the box length. The distance is divided into bins and any time the distance between two particles is calculated, it is put into the relevant bin. In the end total number of bins is normalized and final result is plotted in Fig 2.2.

We compared our pair distribution function with the one in Fig 4 in the paper of McMillan and observed good agreement.

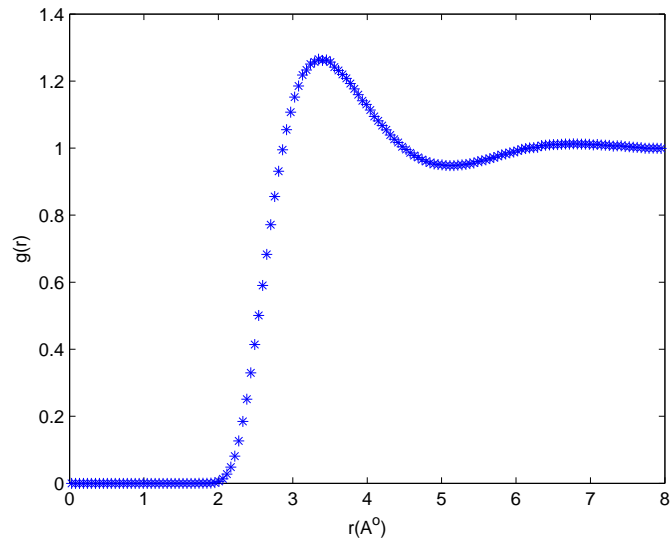


Figure 2.2: The pair distribution function for the 3 dimensional liquid Helium4 for the variational parameter $a_1=2.6$ and $a_2=5$

2.2.2 VMC Study of 2 Dimensional Liquid He4

The ground state energy per particle of two dimensional Helium4 liquid and solid is calculated by Liu et al. in 1977 by using a very similar wave function that Mcmillan used. The Wave function is written as below with the σ as the unit of the length.

$$\psi_L = \exp \left[-\frac{1}{2} \left(\frac{b}{r} \right)^5 \right] \quad (2.23)$$

where b is the variational parameter. The same calculations are done in order to calculate the ground state energy and the pair distribution function with the optimal value of b which is 1.15; $b=1.25$. We have calculated properties of the system for $b=1.2$. The energy plot for the liquid system is drawn with respect to different density values and one can see the good qualitative and quantitative agreement with the Fig.1 of the Liu et al [2].

The pair distribution function of the 2 Dimensional system for $\rho\sigma^2=0.4$ and $\rho\sigma^2=0.234$ is plotted below and again very good qualitative agreement is observed with the Fig.2 of Liu et al. One can observe from the pair distribution functions

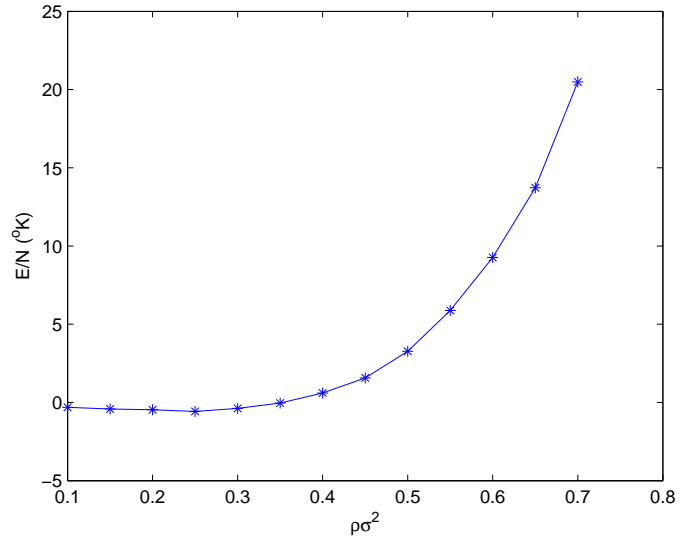


Figure 2.3: The energy plot for the 2 dimensional liquid Helium4 for $b=1.2$

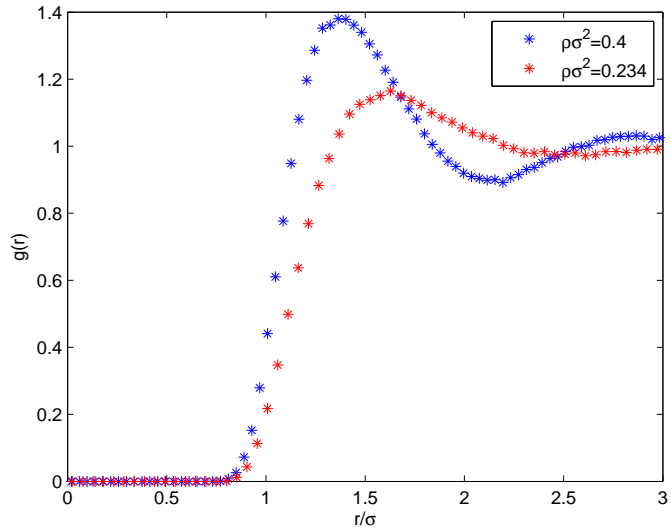


Figure 2.4: The pair distribution function of the 2 dimensional liquid Helium4 for the density values of $\rho\sigma^2=0.4$ and for $\rho\sigma^2=0.234$ for $b=1.2$

for these two different densities that as the density increases the solidification starts to be more favorable for 2D boson system. However, Liu et al. calculated the energies of the crystal phase for 2D bosons for different densities and they plotted the energy diagram in the Fig 1 of their paper. They observed that the ground state for 2D boson system is liquid phase.

Those derivations were in order to test the correctness of the code to be used in the charged systems. We obtained very good results from our tests so we decided to pass to the 2D charged systems.

Chapter 3

Ewald Summation and Natori-Ceperley Method

Simulations of real large systems consisting of particle numbers on the order of 10^{23} are difficult to perform since present technology computers are able to handle on the order of thousands particles at most [22]. Since it is not enough to mimic the bulk with that many atoms boundary conditions are fixed. Usually in Molecular Dynamics (MD) and Monte Carlo (MC) periodic boundary conditions (PBC) are used to handle this problem [22]. In PBC, there is one main cell with fixed number of particles and the space is filled with the replicas of this cell so when one particle is moved its image in the next cell replaces it [22]. The particles in the main cell interact with other particles in the main cell and in the other cells and also with their images in other cells. If the interaction is short-range meaning the tail of the interaction potential dies off after some cut-off, one can ignore the interactions of particles with the ones in other cells so the simulation is done in the main cell only which is called the minimum image convention [22]. However, molecular interactions in real systems like Coulomb are usually long-range that is the tail of the interaction potential can not be ignored by setting a cut-off so the minimum image convention cannot be applied. For example, the potential energy of a periodic system consisting of charged particles can be written

$$U = \frac{1}{2} \sum_{\mathbf{n}}' \sum_{i=1}^N \sum_{j=1}^N \frac{q_i q_j}{|\mathbf{r}_{ij} + \mathbf{n}|} \quad (3.1)$$

where $\mathbf{n} = n_x L_x + n_y L_y + n_z L_z$ representing the translation vectors of the replicas, n_x, n_y, n_z are integers and L_x, L_y, L_z are the sizes of the simulation cell in x,y,z directions. The prime indicates that $i=j$ summation is ignored when $\mathbf{n} = 0$.

In order to evaluate long-range potentials in periodic charge neutral systems the Ewald summation was formulated by Paul Peter Ewald in 1921 [24]. In this thesis potential energies were calculated using Ewald Sums.

3.1 Ewald Sum

The main idea of the Ewald sum is to separate the long-range Coulomb potential into one long-range Fourier sum and one very fast decaying short-range part. The novel physical scenario behind this mathematical trick is that each δ function charge decaying with $1/r$ is now surrounded by a gaussian charge cloud which has minus the total charge of the original δ function charge so that now δ function charge is screened by the charge cloud and is effectively fast decaying [22]. To correct for the added charge distribution another gaussian charge distribution with charge equal to the original δ function is added so that in the system there is a periodic function of gaussian charge clouds which can be represented by Fourier sums [22]. An important correction must be done due to the interaction of the δ function charge with its own charge cloud added for background [22].

The Ewald Summation in the quasi two dimensional system with finite extension in z-direction can be found elsewhere [22] and can be formulated as below

$$U = U_{sr} + U_{lr} + U_{k=0} + U_{self} \quad (3.2)$$

where U_{sr} is the short-range part, U_{lr} is the long-range part, $U_{k=0}$ is the $k=0$ term and U_{self} is the taken out self interaction part of the summation. Each term can be written as

$$U_{sr} = \frac{1}{2} \sum_{i=1}^N \sum_{j=1}^N \sum_{\mathbf{m}=\mathbf{0}}^{\infty} \frac{q_i q_j \text{erfc}(\alpha |\mathbf{r}_{ij} + \mathbf{m}|)}{\alpha |\mathbf{r}_{ij} + \mathbf{m}|} \quad (3.3)$$

$$U_{lr} = \frac{\pi}{2V} \sum_{i=1}^N \sum_{j=1}^N \sum_{\mathbf{k} \neq \mathbf{0}} q_i q_j \frac{\cos(\mathbf{k} \cdot \mathbf{r}_{ij})}{k} \quad (3.4)$$

$$\times \left\{ \exp(kz_{ij}) \text{erfc}\left(\alpha z_{ij} + \frac{k}{2\alpha}\right) + \exp(-kz_{ij}) \text{erfc}\left(-\alpha z_{ij} + \frac{k}{2\alpha}\right) \right\}$$

$$U_{k=0} = -\frac{\pi}{V} \sum_{i=1}^N \sum_{j=1}^N q_i q_j \left\{ z_{ij} \text{erf}(\alpha z_{ij}) + \frac{1}{\alpha \sqrt{\pi}} \exp(-\alpha^2 z_{ij}^2) \right\} \quad (3.5)$$

$$U_{self} = -\frac{\alpha}{\sqrt{\pi}} \sum_{i=1}^N q_i^2 \quad (3.6)$$

3.2 Natoli-Ceperley Method

Evaluation of long-range potentials in periodic systems requires careful treatment as explained in the Ewald Method section. Since the tail of the potential does not die out at long distances, one should consider the interaction of the particles with its images too. If we have a long ranged potential $V(\mathbf{r})$ where \mathbf{r} is the distance between two particles in the simulation cell

$$V_{pp} = \sum_{\mathbf{l}} V(\mathbf{r} + \mathbf{l}) \quad (3.7)$$

where $\mathbf{l} = n_x L_x + n_y L_y + n_z L_z$, n_x, n_y, n_z are integers and L_x, L_y, L_z are the sizes of the simulation cell in x,y,z directions. This periodic potential can be written in Fourier space as explained before as

$$v_{pp} = \sum_{\mathbf{k}} v_{\mathbf{k}} e^{i\mathbf{k} \cdot \mathbf{r}} \quad (3.8)$$

In Ewald summation the convergence of the real and Fourier sums are controlled by an open parameter but in this method the aim is to get those sums optimally without a user defined parameter [25]. Also Ewald sum explained was for the potentials which decay with a power law like coulomb however not all potentials we use in this thesis are in that form. The advantage of this technique is that it helps one to break any kind of potentials into real and Fourier components [25].

We can start by defining an approximate optimized potential as in the form below

$$v_{op} = \sum w(\mathbf{r} + \mathbf{l}) + \sum_{|\mathbf{k}| < K_c} y_{\mathbf{k}} e^{i\mathbf{k} \cdot \mathbf{r}} \quad (3.9)$$

where $w(\mathbf{r})$ is the real space part of the approximate potential and it vanishes at the boundaries of the simulation cell.

$$w(\mathbf{r}) \equiv 0 \text{ for } r > R_c \quad (3.10)$$

To minimize the error, one can minimize the mean squared difference between the approximate optimal potential and the periodic exact potential as shown below

$$\chi^2 = \frac{1}{V} \int d\mathbf{r} [v_{pp}(r) - v_{op}(r)]^2 \quad (3.11)$$

after some arrangement one can write the mean squared difference in two sums

$$\chi^2 = \sum_{|\mathbf{k}| < K_c} (v_{\mathbf{k}} - y_{\mathbf{k}} - w_{\mathbf{k}})^2 + \sum_{|\mathbf{k}| > K_c} (v_{\mathbf{k}} - w_{\mathbf{k}})^2 \quad (3.12)$$

by setting the first term to zero one can get the optimal y_k values as

$$y_{\mathbf{k}} = v_{\mathbf{k}} - \sum_i t_i c_{i\mathbf{k}} \text{ for } |\mathbf{k}| \leq K_c \quad (3.13)$$

where

$$c_{i\mathbf{k}} = \frac{1}{V} \int_0^{r_c} d\mathbf{r} e^{-i\mathbf{k}\cdot\mathbf{r}} c_i(r) \quad (3.14)$$

we can expand the real space function in some basis functions $c_i(\mathbf{r})$

$$w(\mathbf{r}) = \sum_i t_i c_i(\mathbf{r}) \quad (3.15)$$

After setting the first part to zero to determine $y_{\mathbf{k}}$, the integral in equation 3.11 becomes

$$\chi^2 = \frac{1}{V} \int d\mathbf{r} \left(\sum_{|\mathbf{k}| > K_c} e^{i\mathbf{k}\cdot\mathbf{r}} (v_{\mathbf{k}} - \sum_i c_{i\mathbf{k}} t_i) \right)^2 \quad (3.16)$$

By expanding the squared term we get

$$\chi^2 = \frac{1}{V} \int d\mathbf{r} \left(\sum_{|\mathbf{k}| > K_c} \sum_{|\mathbf{k}'| > K_c} e^{i\mathbf{k}\cdot\mathbf{r}} e^{-i\mathbf{k}'\cdot\mathbf{r}} (v_{\mathbf{k}} - \sum_i c_{i\mathbf{k}} t_i) (v_{\mathbf{k}'} - \sum_{i'} c_{i'\mathbf{k}'} t_{i'}) \right) \quad (3.17)$$

To find the optimal t_i values, the first derivative of the χ^2

$$\frac{\partial \chi^2}{\partial t_{i'}} = \frac{2}{V} \int d\mathbf{r} \left(\sum_{|\mathbf{k}| > K_c} \sum_{|\mathbf{k}'| > K_c} e^{i\mathbf{k}\cdot\mathbf{r}} e^{-i\mathbf{k}'\cdot\mathbf{r}} (-v_{\mathbf{k}} + \sum_i c_{i\mathbf{k}} t_i) c_{i'\mathbf{k}'} \right) \quad (3.18)$$

Integration of the exponential result in δ function so the final expression for the derivative of the χ^2 becomes as follows

$$\frac{\partial \chi^2}{\partial t_{i'}} = 2 \left(\sum_{|\mathbf{k}| > K_c} (-v_{\mathbf{k}} + \sum_i c_{i\mathbf{k}} t_i) c_{i'\mathbf{k}'} \right) \quad (3.19)$$

By setting the derivative to zero the final set of equations can be written as

$$\sum_n \sum_{|\mathbf{k}| > K_c} c_{i\mathbf{k}} c_{n\mathbf{k}} t_n = \sum_{|\mathbf{k}| > K_c} v_{\mathbf{k}} c_{i\mathbf{k}} \quad (3.20)$$

The mean squared error in the optimization procedure can be found easily from the integration and can be calculated as

$$\chi^2 = \sum_{|\mathbf{k}| > K_c} y_{\mathbf{k}}^2 \quad (3.21)$$

Up to this point the main steps are explained for a general interpolating function c_i . Both in the paper of Natoli and Ceperley [25] and in this thesis locally piecewise-quintic Hermite interpolants (LPQHI) are used as basis functions. They are used to form the long ranged part of the potential.

3.2.1 LPQHI

For the interpolation procedure, one divides the real space cut-off which is half of the simulation box length into $m+1$ knots so if the distance between the knots is δ then $R_c = m\delta$ [25]. Since the LPQHI basis functions have two derivatives c_i becomes $c_{i\alpha}$ so t_i is now $t_{i\alpha}$ where $0 \leq \alpha \leq 2$ where α indicating the derivative number [25]. LPQHI basis functions can be written as follows where i indicates the knot number as below

$$c_{i\alpha}(r) = \begin{cases} (\Delta)^\alpha \sum_{n=0}^5 M_{\alpha n} \left(\frac{r-r_i}{\Delta}\right)^n & , r_i < r < r_{i+1} \\ (-\Delta)^\alpha \sum_{n=0}^5 M_{\alpha n} \left(\frac{r_i-r}{\Delta}\right)^n & , r_{i-1} < r < r_i \\ 0 & , otherwise \end{cases} \quad (3.22)$$

where the M matrix is

$$M = \begin{bmatrix} 1 & 0 & 0 & -10 & 15 & -6 \\ 0 & 1 & 0 & -6 & 8 & -3 \\ 0 & 0 & 0.5 & -1.5 & 1.5 & -0.5 \end{bmatrix} \quad (3.23)$$

In the figure 3.1 one can see the basis functions for any knot value. Fourier transforms of the basis functions to be used in equation 3.14 are calculated as

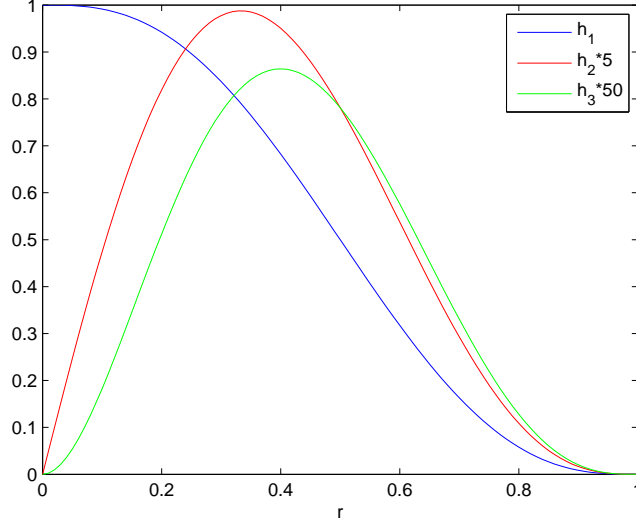


Figure 3.1: The LPQHI (locally piecewise quintic Hermite interpolants) and its derivatives

$$c_{i\alpha k} = \frac{1}{V} \int_0^{r_c} d\mathbf{r} e^{-i\mathbf{k}\cdot\mathbf{r}} c_{i\alpha}(r) \quad (3.24)$$

one can write it in a more compact form as follows

$$c_{i\alpha k} = (\Delta)^\alpha \sum_{n=0}^5 M_{\alpha n} (D_{ikn}^+ + D_{ikn}^- (-1)^{\alpha+n}) \quad (3.25)$$

where

$$D_{ikn}^\pm = \pm \frac{1}{V} \int_{r_i}^{r_{i\pm 1}} d\mathbf{r} e^{-i\mathbf{k}\cdot\mathbf{r}} \left(\frac{r - r_i}{\Delta}\right)^n \quad (3.26)$$

Since coulomb potential has singularity at the origin it is possible to impose it into the LPQHI basis functions as follows

$$c_{i\alpha}(r) = \frac{1}{r} \sum_{n=0}^5 M_{\alpha n} \left(\frac{r - r_i}{\Delta}\right)^n \quad (3.27)$$

3.2.2 Two Dimensional Optimized Coulomb

In two dimensions it is known that the Ewald formula for the Coulomb potential is divided in real and Fourier space terms as below [3]

$$w(\mathbf{r}) = q \frac{\text{erfc}(\alpha r)}{r} \quad (3.28)$$

$$y_k = \left\{ \begin{array}{ll} \frac{2\pi}{V} \frac{\text{erfc}(k/2\alpha)}{k} & , k \neq 0 \\ -\frac{2\sqrt{\pi}}{\alpha V} & , k = 0 \end{array} \right\} \quad (3.29)$$

One can use Natoli-Ceperley treatment of longed range functions in two dimensions after some little manipulation of the functions. For example, since the definition of the Bessel function is as follows

$$J_0(x) = \frac{1}{2\pi} \int_0^{2\pi} e^{ix \sin(\theta)} d\theta \quad (3.30)$$

in two dimensions one can write the functions in equation 3.20 as

$$D_{ikn}^{\pm} = \pm \frac{2\pi}{V} \int_{r_i}^{r_{i\pm 1}} dr J_0(r) r \left(\frac{r - r_i}{\Delta} \right)^n \quad (3.31)$$

To solve the equation 3.14 singular value decomposition (SVD) is used. The unknown $t_{n\alpha}$ constants were obtained by using Gnu Scientific Library SVD function.

To compare our results with the ones of Holzmann et al. [3] we used $N_{\text{spline}} = 2$ for interpolation. Also $K_c = 4\pi/L$ which corresponds to 4 shells so 13 k points in k-space. The short range part of the potential can be written as

$$y(r) = \frac{q}{r} [y_0 + 2y_1 (\cos(\frac{2\pi}{L}x) + \cos(\frac{2\pi}{L}y)) + 4y_2 \cos(\frac{2\pi}{L}x) \cos(\frac{2\pi}{L}y) + 2y_4 (\cos(\frac{4\pi}{L}x) + \cos(\frac{4\pi}{L}y))] \quad (3.32)$$

where y_n s represent the short range values for each shell n . We have tabulated our y_n values and the ones in Holzmann et al. [3] as y_{nH} in the table below

Table 3.1: Our results and results from Holzmann et al. for y_k values for $N_{spline} = 2$ and $K_c = 4\pi/L$

n	0	1	2	4
y_n	-0.87165	0.26181	0.071408	0.0047449
y_{nH}	-0.870938	0.262177	0.0715766	0.00474028

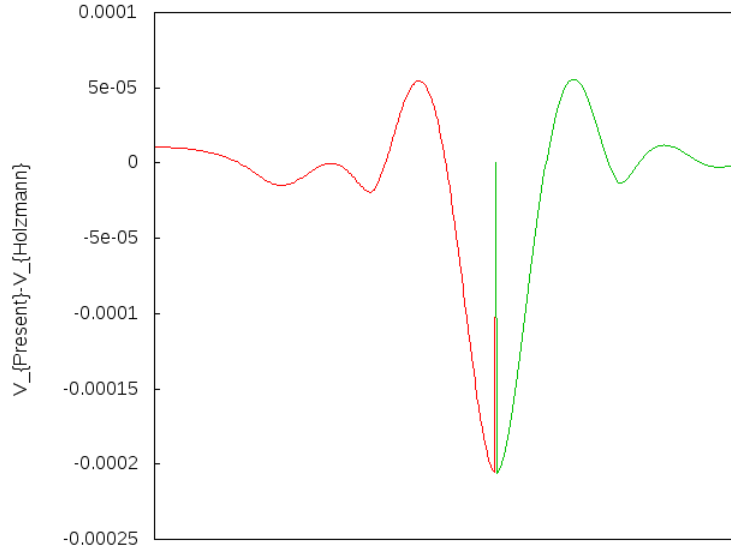


Figure 3.2: The difference between the optimized potential of ours and the one of Holzmann et al. :Red one is the difference between the potentials through the corner of the box and green one is the difference through the middle of the box length

The calculated mean squared difference between the periodic potential and the optimized potential, χ^2 is on the order of 10^{-8} .

The total potential can be calculated by using equation 3.3. In the figure below we plotted the difference between total potential of Holzmann et al. [3] and ours. We calculated the difference between our results and Holzmann et al. both in the direction of the corner of the box and middle of the square side.

In Fig.3 of Holzmann et al. [3] one can see that the difference between the periodic potential evaluated by using many replicated cells and the optimized one is not very stable since both the number of splines and the number of k-space points are not enough to get a good representation. However, again from the same figure one can see that when the cut-off is increased the difference becomes

less and more stable.

We obtained a good representation of the long-range Coulomb potential in the simulation cell. Therefore, In the rest of the thesis we have used the same interpolation structure while evaluating long-range pseudo potentials.

Chapter 4

Two Dimensional Charged Bose Gas

4.1 Electron Gas

The electron gas is a system where there are electrons interacting with each other and with the uniform background which cancels the total charge of the electrons so the system of interest is neutral. Under the assumption that electron-electron and electron-background interactions cancel each other the Hamiltonian of the electron gas can be written as follows [26]

$$H = \frac{1}{r_s^2} \sum_{1 \leq i \leq N} \nabla_i^2 + \frac{2}{r_s} \sum_{1 \leq i < j \leq N} \frac{1}{|\mathbf{r}_i - \mathbf{r}_j|} \quad (4.1)$$

where the length unit of the system is a and defined by the dimensionless parameter $r_s = a/a_0$ where a_0 is the Bohr radius and the energy unit is Ry(Rydberg) where $1 \text{ Ry} = me^4/2\hbar^2$ so the density is always $1/\pi$. It can be seen from the Hamiltonian that the system is liquid when r_s is small since in this case the kinetic term dominates the potential. However, when r_s is large the potential term dominates so the system is more localized like Wigner Crystal (WC).

The wave function of the charged system can be approximated as

$$\psi_T(\mathbf{R}) = D(\mathbf{r}) \exp\left(-\sum_{1 \leq i < j \leq N} u(|\mathbf{r}_i - \mathbf{r}_j|)\right) \quad (4.2)$$

where D is the Slater determinant and it is the multiplication of two separate Slater determinants one for spin-up particles and one for spin-down particles. The function u is a two body function correlating the electrons. This type of wave function is called Slater-Jastrow wave function. The optimal pseudo potential derived by Gaskell [8, 9] called Random Phase Approximation (RPA) pseudo potential is of the form [10]

$$2u_{RPA}(k) = -\frac{1}{S_0(k)} + \left(\frac{1}{S_0(k)^2} + \frac{4v(k)m}{\hbar^2 k^2}\right)^{1/2} \quad (4.3)$$

where $S_0(k)$ is the static structure factor for electronic system. The real space form of any function in k space can be obtained by the transformation

$$u(\mathbf{k}) = \rho \int_0^L d\mathbf{r} e^{i\mathbf{k}\cdot\mathbf{r}} u(\mathbf{r}) \quad (4.4)$$

for example, for Coulomb interaction the r -space transform is written as below

$$v(k) = \frac{2\pi e^2}{k} \text{ for } v(r) = \frac{1}{r} \quad (4.5)$$

For the electronic system the static structure factor in two dimension is formulated as follows

$$S_0(k) = \frac{2}{\pi} \left(\sin^{-1}\left(\frac{k}{2k_F}\right) + \frac{k}{2k_F} \left(1 - \frac{k^2}{4k_F^2}\right)^{1/2} \right) \quad (4.6)$$

where $k_F = \sqrt{2}$ is the fermi wave vector for unpolarized system.

The optimal pseudo potential satisfies the cusp condition which is the condition when two electrons approach each other and the long range form as below

$$\lim_{r \rightarrow 0} \left(\frac{du(r)}{dr} \right) = -r_s \text{ and } \lim_{r \rightarrow \infty} (u(r)) = 1.48 \left(\frac{r_s}{r} \right)^{1/2} \quad (4.7)$$

Special techniques to evaluate the determinants and the matrix updates for the VMC calculations of the electronic system is explained in detail in the paper of Ceperley (1977) [27].

Up to now the aim was to introduce the fundamental properties of the wave function to be used in VMC calculations and the optimal pseudo potential for correlation of electrons. In the next section we will use the adapted versions of those equations for a system of charged bosons. Our aim for this work is to reproduce the paper of de Palo et al. [4]

4.2 Bose Gas

Bose gas is a system which is composed of charged bosons interacting via coulomb potential. The static structure factor of the non-interacting Bose system is given by $S_0 = 1$. We have indistinguishable particles which are spin-0 bosons in two dimensions so we have only Jastrow factor in our wave function.

The pseudo potential $u_{RPA}(r)$ and also the Coulomb potential are both long range so Ewald summation and Natoli-Ceperley process was performed to fit them into the simulation box as explained in the previous chapter. For Ewald summation we have used r_c as half of the box length and we have used 50-55 splines to interpolate the Natoli-Ceperley short range part and 57-61 k-points for the long range calculations. The observed value of the mean square difference (χ^2) for Natoli-Ceperley part was on the order of $10^{-14} - 10^{-15}$. The energies of the system are calculated for different number of particles and due to the long-range behaviour of the potentials we observed particle number dependence in the energy results. Therefore, in order to fit the energy values to the infinite system we have used the formula $E_\infty = E_N + a(r_s)/N + b(r_s)/N^2$ as de Palo et al [4] did. The calculated energies for different number of particles and for different density values are tabulated below.

Table 4.1: VMC calculations of potential, kinetic and total energies of the 2D charged bosons for different number of particles and the extrapolated energy results (E_∞) with their standard deviations.

N		$r_s=1$	$r_s=2$	$r_s=5$	$r_s=10$	$r_s=20$	$r_s=40$	$r_s=75$
30	E_K	0.298845	0.154962	0.0547103	0.0216346	0.00792491	0.00279418	0.0010753
	E_V	-1.45953	-0.833216	-0.37419	-0.196114	-0.10106	-0.0516096	-0.0279309
	E_T	-1.16069	-0.678254	-0.319479	-0.17448	-0.0931347	-0.0488154	-0.0268556
40	E_K	0.303502	0.156836	0.0548595	0.0217216	0.00795732	0.00280579	0.00107977
	E_V	-1.46092	-0.833765	-0.373433	-0.195985	-0.101027	-0.0515977	-0.0279269
	E_T	-1.15742	-0.676929	-0.318574	-0.174264	-0.09307	-0.0487919	-0.0268471
60	E_K	0.305733	0.157976	0.0551557	0.0218083	0.00798732	0.00281617	0.00108382
	E_V	-1.45739	-0.833284	-0.373349	-0.195936	-0.101003	-0.0515906	-0.0279247
	E_T	-1.15165	-0.675308	-0.318193	-0.174128	-0.0930159	-0.0487745	-0.0268408
80	E_K	0.30766	0.158073	0.0553006	0.0218511	0.00800096	0.00282095	0.00108574
	E_V	-1.45753	-0.832285	-0.373453	-0.195895	-0.100985	-0.0515881	-0.0279218
	E_T	-1.14987	-0.674212	-0.318152	-0.174043	-0.0929842	-0.0487671	-0.0268361
100	E_K	0.307389	0.158556	0.0552871	0.0218716	0.00800934	0.00282386	0.00108683
	E_V	-1.4548	-0.832417	-0.373195	-0.195871	-0.100973	-0.0515824	-0.0279202
	E_T	-1.14741	-0.673861	-0.317908	-0.173999	-0.0929633	-0.0487585	-0.0268334
120	E_K	0.308029	0.15865	0.0553786	0.021886	0.0080138	0.00282568	0.00108753
	E_V	-1.45476	-0.832025	-0.373245	-0.195863	-0.100981	-0.0515787	-0.0279189
	E_T	-1.14673	-0.673375	-0.317866	-0.173977	-0.092967	-0.048753	-0.0268313
150	E_K	0.308976	0.158574	0.0553942	0.0218982	0.00801876	0.00282719	0.00108811
	E_V	-1.45538	-0.831711	-0.373107	-0.195835	-0.100965	-0.0515801	-0.0279197
	E_T	-1.1464	-0.673137	-0.317712	-0.173937	-0.0929463	-0.0487529	-0.0268316
180	E_K	0.308517	0.158499	0.0553983	0.0219063	0.00802152	0.00282823	0.00108857
	E_V	-1.45382	-0.831174	-0.373126	-0.19583	-0.100966	-0.0515784	-0.0279177
	E_T	-1.14531	-0.672675	-0.317728	-0.173924	-0.0929441	-0.0487501	-0.0268292
200	E_K	0.308909	0.158621	0.0554235	0.0219095	0.00802266	0.0028288	0.00108877
	E_V	-1.45436	-0.831201	-0.373142	-0.195842	-0.100962	-0.0515769	-0.0279178
	E_T	-1.14546	-0.67258	-0.317718	-0.173933	-0.0929395	-0.0487481	-0.026829
	E_∞	-1.14239	-0.671322	-0.31756	-0.173855	-0.0929117	-0.0487381	-0.0268242
	E_{std}	± 0.0005812	± 0.0001278	$\pm 9.816 \times 10^{-5}$	$\pm 1.338 \times 10^{-5}$	$\pm 5.879e \times 10^{-6}$	$\pm 2.103 \times 10^{-6}$	$\pm 9.1137 \times 10^{-7}$

We have tabulated some charged Bose calculations done before for comparison as de Palo et al. did. The HNC (hypernetted-chain approximation) calculations are done by Apaja et al. [16], STLS calculations are performed by Gold [17] and STW are done by Sim, Tao and Wu [18]. We observed good agreement between our results and the VMC results of de Palo et al.

The pair distribution function of 2D Bose system is plotted for different values of density as below and again at least good qualitative agreement is observed between ours and the one of de Palo et al [4]. As density increases the formation

Table 4.2: Energy results of de Palo et al for VMC, DMC calculations, our VMC calculations, STLS, STW and HNC calculations

r_s	E_{dePalo}^{DMC}	E_{dePalo}^{VMC}	$E_{Present}^{VMC}$	HNC	STW	STLS
1	-1.1448(5)	-1.14269(7)	-1.1423(5)	-1.1458	-1.1062	-
2	-0.6740(2)	-0.67192(6)	-0.6713(1)	-0.6740	-0.6631	-0.6484
5	-0.31903(5)	-0.317456(6)	-0.31756(9)	-0.3185	-0.3133	-0.3078
10	-0.17480(5)	-0.17385(3)	-0.17385(1)	-0.1741	-0.16685	-0.1724
20	-0.093387(8)	-0.092903(3)	-0.092911(5)	-0.0928	-0.086024	-0.0959
40	-0.048986(8)	-0.048737(2)	-0.048738(2)	-	-	-
75	-0.026965(6)	-0.0268246(8)	-0.0268242(9)	-	-	-

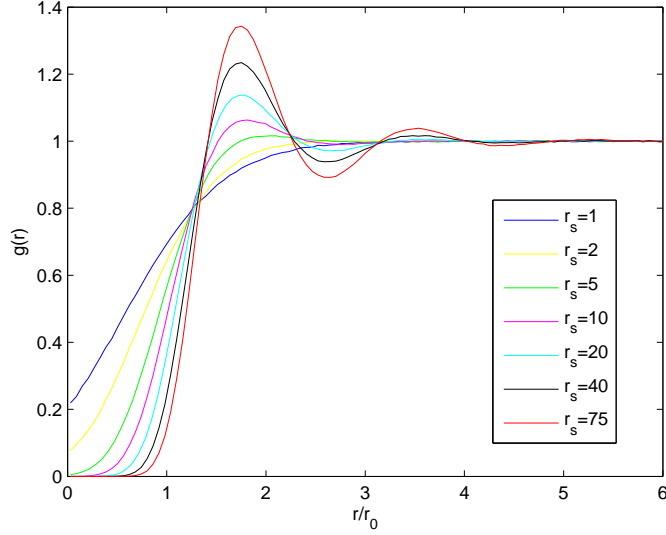


Figure 4.1: The pair distribution function of 2D charged boson system for $r_s=1,2,5,10,20,40,75$

of peaks signals the tendency of the system for the crystallization.

In the paper of de Palo et al. the ground state energies of DMC calculations are fit to a function:

$$E_g(r_s) = -[a_0 r_s^{b_0} + a_1 r_s^{b_1} + a_2 r_s^{b_2} + a_3 r_s^{b_3}]^{-c} \quad (4.8)$$

where $a_0=0.2297$, $a_1=0.161$, $a_2=0.0594$, $a_3=0.01017$, $b_1=94/21$, $b_2=73/14$, $b_3=40/7$, $c=7/40$.

The competition of kinetic and potential energies result in a phase transition from liquid to crystal as r_s increases since at lower densities the coulomb potential

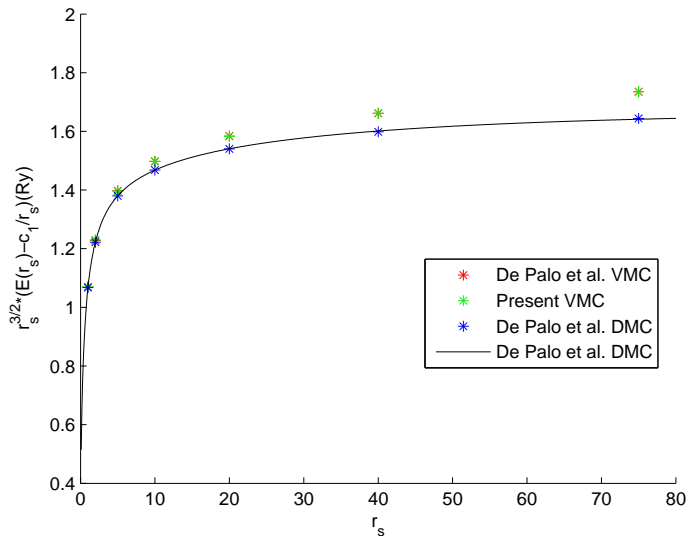


Figure 4.2: The energy plot VMC,DMC results for $r_s^{3/2} * (E(r_s) - c_1/r_s)$ where $c_1=-2.2122$ is the madelung constant for 2D lattice

leads localization. In order to investigate the crystallisation of 2D fermion system Rapisarda et al. did some calculations for the ground state energy [28] and they observed that fermions crystallize at $r_s=34$. They fitted the crystal energies by using the formulation of Tanatar and Ceperley [11].

$$E(r_s) = \frac{c_1}{r_s} + \frac{c_{\frac{3}{2}}}{r_s^{3/2}} + \frac{c_2}{r_s^2} \quad (4.9)$$

where the coefficients are calculated as $c_1=-2.20943$, $c_{\frac{3}{2}}=1.58948$ and $c_2=0.146762$.

We plotted the Fig.1 of de Palo et al. with the inclusion of our VMC results. The parametrization is done by excluding the Madelung constant $c_1=-2.2122$ and the new function $r_s^{3/2} * (E(r_s) - c_1/r_s)$ is plotted below in the unit pf Rydberg where c_1 is the Madelug term. In the Fig. 4.2 we plotted the energy values from our calculations and the ones of DMC,VMC calculations of de Palo et al. with the inclusion of DMC fitting function given in equation 1 of de Palo et al. And also in Fig. 4.3 we included the WC calculations done by Rapisarda et al [28]. From the plot one can see that the ground state energy of 2D boson system for WC (Wigner Crystal) is more favorable than the liquid. We are comparing crystal data of fermion with the boson data. The reason behind is that there is

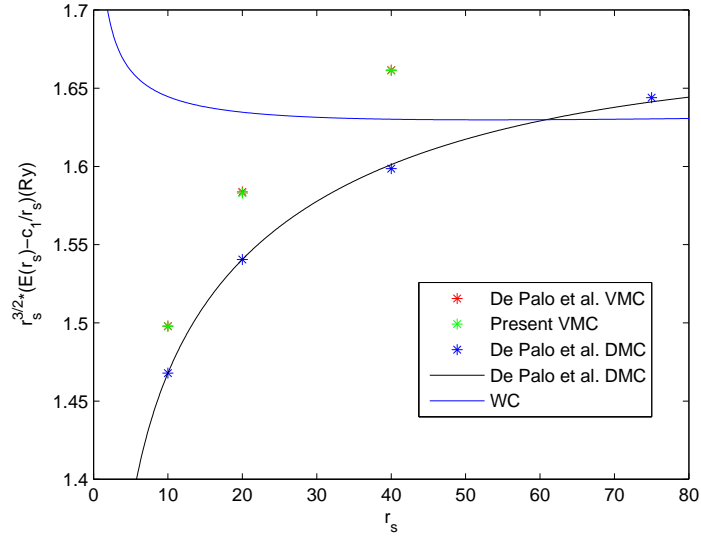


Figure 4.3: The energy plot VMC,DMC results and for the WC calculations by Rapisarda et al. for $r_s^{3/2} * (E(r_s) - c_1/r_s)$ where $c_1=-2.2122$ is the madelung constant for 2D lattice

no available boson calculations on lattice and also when the system is lattice the behaviour of fermions is similar to bosons due to the fact that they sit on the lattice points so they are not effected by Pauli exclusion principle.

From the graph it can be seen that the phase transition points for VMC and DMC calculation is different. For VMC results the phase transition seems to occur at $r_s \simeq 30$ whereas for DMC calculation it is about $r_s=60$. Since DMC is an exact method the correct phase transition value of r_s is expected to be the one given by DMC calculation. Also the pair distribution function we plotted for our VMC calculations shows that VMC is not able to capture the peaks at large r_s values whereas it is more similar to DMC results at small r_s values.

Chapter 5

Projected Wave Functions

5.1 Kinetic Energy Projection of RPA Wave Function

In this chapter our aim is to see whether or not we can obtain better energy values by optimizing the RPA pseudo potential via introducing a kinetic energy projection with a variational parameter to the wave function. If we define the new wave function of our system as $\tilde{\psi}$ and the RPA wave function as ψ , we can write it as

$$|\tilde{\psi}\rangle = e^{\alpha\hat{T}}|\psi\rangle \quad (5.1)$$

After this rearrangement the expectation values of any observable in our system will be evaluated as

$$\langle \hat{A} \rangle = \frac{\langle \tilde{\psi} | \hat{A} | \tilde{\psi} \rangle}{\langle \tilde{\psi} | \tilde{\psi} \rangle} \quad (5.2)$$

We can introduce coordinate identities to our system and the normalization of our new wave function can be calculated as

$$\langle \tilde{\psi} | \tilde{\psi} \rangle = \int d\mathbf{x}_L d\mathbf{x}_R \langle \psi | x_L \rangle \langle x_L | e^{2\alpha\hat{T}} | x_R \rangle \langle x_R | \psi \rangle \quad (5.3)$$

and we can re express it as

$$\langle \tilde{\psi} | \tilde{\psi} \rangle = \int d\mathbf{x}_L d\mathbf{x}_R \psi(x_L) \langle x_L | e^{2\alpha\hat{T}} | x_R \rangle \psi(x_R) \quad (5.4)$$

The expression includes a quantity called Propagator which is the probability amplitude of a move from a point to another one [29] and can be written as

$$K = \langle x_L | e^{2\alpha\hat{T}} | x_R \rangle \quad (5.5)$$

We can introduce momentum identities so we have

$$K = \int d\mathbf{k} \langle x_L | k \rangle \langle k | e^{2\alpha\hat{T}} | k \rangle \langle k | x_R \rangle \quad (5.6)$$

by evaluating the product of momentum and real space eigenvectors we obtain

$$K = \frac{1}{2\pi} \int d\mathbf{k} \exp(i\mathbf{k} \cdot \mathbf{x}_L) \langle k | e^{2\alpha\hat{T}} | k \rangle \exp(-i\mathbf{k} \cdot \mathbf{x}_R) \quad (5.7)$$

The final form of the Propagator can be written as

$$\begin{aligned} K &= \frac{1}{2\pi} \int d\mathbf{k} \exp(i\mathbf{k} \cdot (\mathbf{x}_L - \mathbf{x}_R)) \exp(-\alpha\hbar^2 k^2 / (2m)) \\ &= \sqrt{\frac{m}{4\pi\hbar^2\alpha}} \exp\left(\frac{-m}{4\alpha\hbar^2} (x_L - x_R)^2\right) \end{aligned} \quad (5.8)$$

In order to use this new form of the wave function in our code we converted the unit of it to our unit system as

$$K = \sqrt{\frac{r_s^2}{8\pi\alpha}} \exp\left(\frac{-r_s^2}{8\alpha} (x_L - x_R)^2\right) \quad (5.9)$$

With the inclusion of the Propagator, the normalization we formulated in equation 5.3 can be written as follows

$$\langle \tilde{\psi} | \tilde{\psi} \rangle = \int d\mathbf{x}_L d\mathbf{x}_R \sqrt{\frac{r_s^2}{8\pi\alpha}} \psi(x_L) \psi(x_R) \exp\left(\frac{-r_s^2}{8\alpha} (x_L - x_R)^2\right) \quad (5.10)$$

In our new normalization function we have Gaussian terms which contribute too much to the integral and make the pseudo potential contribution negligible. This leads a very small amount of acceptance ratio so we applied Metropolis-Hasting method at this point by introducing Gaussian deviates.

A Gaussian function with a standard deviation σ and mean of the distribution μ can be written as follows

$$\frac{1}{\sigma\sqrt{2\pi}} \exp\left(-\frac{(x-\mu)^2}{2\sigma^2}\right) dx = du \quad (5.11)$$

In our new MC approach, the aim is to find $x(u)$ where u is distributed according to uniform distribution [22]. The generation of random Gaussian numbers are first introduced by Box and Müller in 1958 [30]. We have used the `gsl_ran_gaussian()` function in the GNU Scientific Library which can provide Gaussian random numbers for any σ and μ . For the normalization above we used Gaussian deviates from $\sigma = 2\alpha/r_s$ and $\mu=0$.

In order to find the expectation values of any operator \tilde{A} diagonal in real space using this technique one can introduce another coordinate x_C which is the coordinate of the particles in the center slab

$$\langle \hat{A} \rangle = \int d\mathbf{x}_R d\mathbf{x}_L d\mathbf{x}_C F(x_L, x_R, x_C) \quad (5.12)$$

$$\begin{aligned} F(x_L, x_R, x_C) = & \langle \psi | x_L \rangle \langle x_L | e^{-\alpha\tilde{T}} | x_C \rangle \langle x_C | e^{-\alpha\tilde{T}} | x_L \rangle \langle x_L | \psi \rangle \\ & \times \frac{\langle x_C | \tilde{A} | x_C \rangle}{\int d\mathbf{x}_L d\mathbf{x}_R \langle \psi | x_L \rangle \langle x_L | e^{2\alpha\tilde{T}} | x_R \rangle \langle x_R | \psi \rangle} \end{aligned} \quad (5.13)$$

By applying the same formulation in order to obtain the Propagator as we did for normalization we can write the expectation value of the operator as

$$\begin{aligned} F(x_L, x_R, x_C) = & \frac{r_s^2}{4\pi\alpha} \psi(x_L) \psi(x_R) \exp\left(\frac{-r_s^2}{4\alpha}(x_L - x_C)^2\right) \exp\left(\frac{-r_s^2}{4\alpha}(x_R - x_C)^2\right) \\ & \times \frac{\langle x_C | \tilde{A} | x_C \rangle}{\int d\mathbf{x}_L d\mathbf{x}_R \sqrt{\frac{r_s^2}{8\pi\alpha}} \psi(x_L) \psi(x_R) \exp\left(\frac{-r_s^2}{8\alpha}(x_L - x_R)^2\right)} \end{aligned} \quad (5.14)$$

The exponential terms can be written as

$$\exp\left(-\frac{r_s^2}{4\alpha}(x_L^2 + x_R^2 + 2x_C^2 - 2x_C(x_L + x_R))\right) \quad (5.15)$$

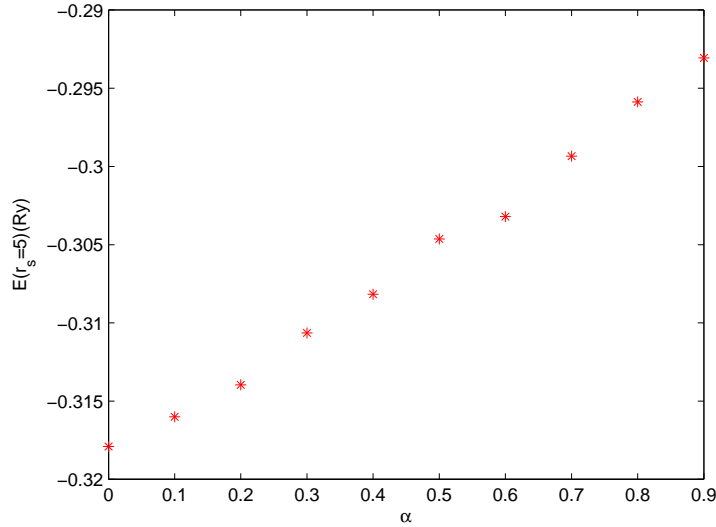


Figure 5.1: The energy values of 2D boson system with a projected wave function for different values of projection coefficient α for the density $r_s=5$

we can eliminate square of the x_L and x_R terms since they are already Gaussian and again in order to make transformation above we can set the central coordinate as $x_C = x_{avg} + \delta$ where $x_{avg} = (x_L + x_R)/2$ and δ is a Gaussian deviate chosen according to Gaussian distribution with $\sigma = \alpha/r_s$ and $\mu = 0$.

The physical scenario behind our method is that we have 3 slabs in which we have our particles. We have one left slab with coordinates x_L, y_L , one right slab with coordinates x_R, y_R and one center slab with coordinates x_C, y_C since we have 2D system. The center slab is connected to the other ones with harmonic springs and the spring constants are proportional to α .

We have calculated energy values for 100 particles for different density values $r_s=5,20,40,75$. The $\alpha=0$ value is the original de Palo calculation from our 2D boson code for 100 particles. The energy plots are below

It can be seen that we are unable to obtain lower energies than the original calculation with optimized RPA pseudo potential since RPA is a very good wave function describing the ground state of the system so it is very difficult to optimize it further.

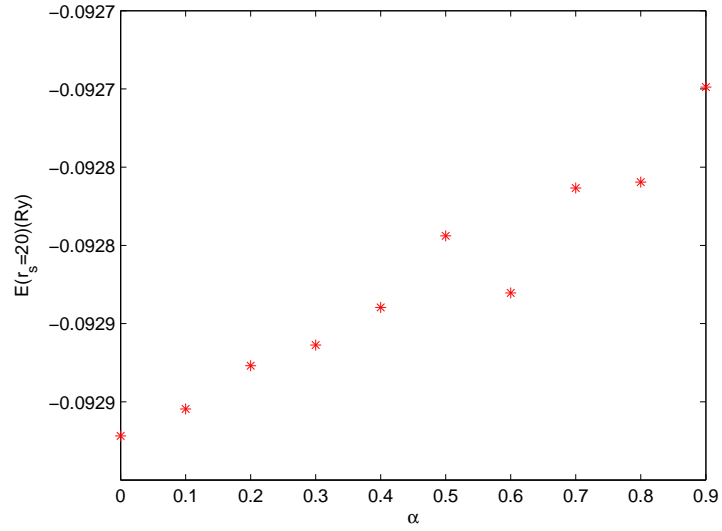


Figure 5.2: The energy values of 2D boson system with a projected wave function for different values of projection coefficient α for the density $r_s=20$

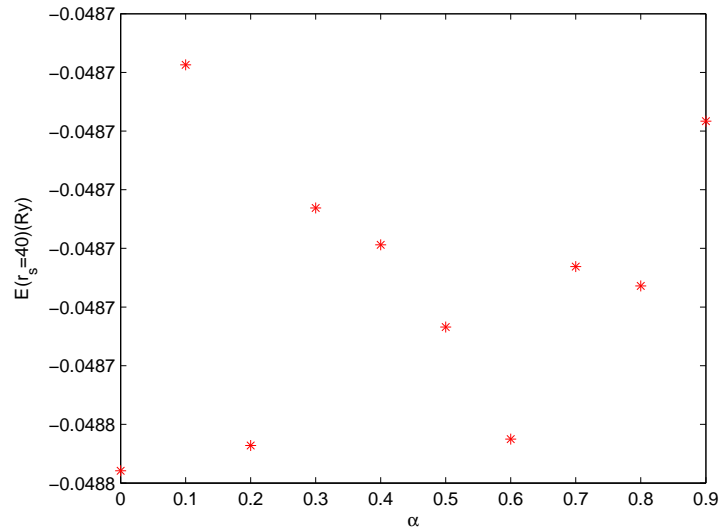


Figure 5.3: The energy values of 2D boson system with a projected wave function for different values of projection coefficient α for the density $r_s=40$

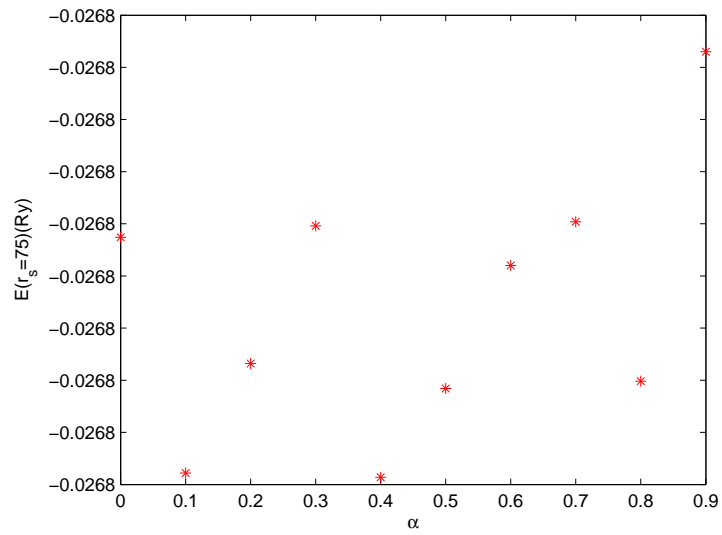


Figure 5.4: The energy values of 2D boson system with a projected wave function for different values of projection coefficient α for the density $r_s=75$

Chapter 6

Conclusion

We studied 2D charged Boson system using Variational Monte Carlo Method. We have started by reproducing the paper of McMillan in which there are Helium4 Bosons interacting via Lennard-Jones potential and its wave function is approximated by a power decaying two body pseudo-potential. We observed very good agreement in the energies and pair distribution functions between our calculations and the ones of McMillan. Then we passed to 2D Helium4 Boson system and reproduce the paper of Liu et al. Again we observed that our energies and pair distribution functions matched to theirs. Since we were going to deal with charged systems we have studied Ewald Summation and Natoli-Ceperley method to evaluate long-range potentials in periodic systems. After reproducing the work of Holzmann et al. we investigated charged Boson system interacting via Coulomb potential. Its wave function is approximated by optimized pseudo-potential derived by Gaskell in 1961. We reproduced the VMC part of de Palo et al. and tried to optimize the pseudo-potential further by introducing kinetic projection to the wave function. However, we observed that we were not able to obtain better energy values. We have concluded our work by obtaining the result that is because optimized pseudo-potential is a very good one so it is very difficult to optimize it more.

Bibliography

- [1] W. McMillan, “Ground state of liquid he4,” *Phys.Rev.*, vol. 138, no. 2A, pp. A442–A451, 1965.
- [2] K. Liu, M. Kalos, and G. Chester, “Ground-state properties of two-dimensional liquid and solid he4,” *Phys.Rev.B*, vol. 13, no. 5, pp. 1971–1974, 1976.
- [3] M. Holzmann and B. Bernu, “Optimized periodic $1/r$ coulomb potential in two dimensions,” *Journal of Computational Physics*, vol. 206, pp. 111–121, 2005.
- [4] S. D. Palo, S. Conti, and S. Moroni, “Monte carlo simulations of two-dimensional charged bosons,” *Phys.Rev.B*, vol. 69, pp. 035109–1–035109–6, 2004.
- [5] D. Pines and P. Nozieres, *The Theory of Quantum Liquids*. Redwood City, CA: Addison-Wesley, 1990.
- [6] D. Bohm and D. Pines, “A collective description of electron interactions: Iii. coulomb interactions in a degenerate electron gas,” *Phys. Rev.*, vol. 92, no. 3, pp. 609–625, 1953.
- [7] D. Bohm and D. Pines, “A collective description of electron interactions: Ii. collective vs individual particle aspects of the interactions,” *Phys. Rev.*, vol. 85, no. 2, pp. 338–353, 1952.
- [8] T. Gaskell, “The collective treatment of many-body systems: 3,” *Proc.Phys.Soc.*, vol. 80, pp. 1091–1100, 1962.

- [9] T. Gaskell, “The collective treatment of a fermi gas: 2,” *Proc.Phys.Soc.*, vol. 77, pp. 1182–1192, 1961.
- [10] D. Ceperley, “Ground state of the fermion one-component plasma: A monte carlo study in two and three dimensions,” *Phys. Rev. B*, vol. 18, no. 7, pp. 3126–3138, 1978.
- [11] B.Tanatar and D. Ceperley, “Ground state of the two-dimensional electron gas,” *Phys. Rev. B*, vol. 39, no. 8, pp. 5005–5016, 1989.
- [12] M. Frank, L. Galeta, T. Hahn, S. Heinemeyer, W. Hollik, H. Rzehak, and G. Weiglein⁵, “Charged higgs boson mass of the mssm in the feynman diagrammatic approach,” *Phys. Rev. D*, vol. 88, pp. 055013–1–055013–20, 2013.
- [13] D. Pugliese, H. Quevedo, and J. A. R. H. R. Ruffini, “Charged boson stars,” *Phys. Rev. D*, vol. 88, pp. 024053–1–024053–19, 2013.
- [14] M. R. Schafroth, “Superconductivity of a charged ideal bose gas,” *Phys. Rev.*, vol. 100, no. 2, pp. 463–475, 1955.
- [15] L. Foldy, “Charged boson gas,” *Phys. Rev.*, vol. 124, no. 3, pp. 649–651, 1961.
- [16] V. Apaja, J. Halinen, E. Krotscheck, and M. Saarela, “Charged boson fluid in two and three dimensions,” *Phys. Rev. B*, vol. 55, no. 19, pp. 12 925–12 945, 1997.
- [17] A. Gold, “Local-field correction of the charged bose condensate for two and three dimensions,” *Z. Phys. B*, vol. 89, pp. 1–10, 1992.
- [18] H. Sim, R. Tao, and F. Wu, “Ground-state energy of charged quantum fluids in two dimensions,” *Phys. Rev. B*, vol. 34, no. 10, pp. 7123–7128, 1986.
- [19] W. Magro and D. Ceperley, “Ground-state properties of the two-dimensional bose coulomb liquid,” *Phys. Rev. Lett.*, vol. 73, no. 6, pp. 826–829, 1994.
- [20] S. Moroni, S. Conti, and M. Tosi, “Monte carlo simulations of the charged boson fluid at t=0,” *Phys. Rev. B*, vol. 53, no. 15, pp. 9688–9696, 1996.

- [21] N. Metropolis, A. Rosenbluth, M. Rosenbluth, A. Teller, and E. Teller, “Equation of state calculations by fast computing machines,” *J. Chem. Phys.*, vol. 21, no. 6, pp. 1087–1092, 1953.
- [22] D. Frenkel and B. Smit, *Understanding Molecular Simulation: From Algorithms and Applications*. San Diego, USA: Academic Press, 1996.
- [23] B. D. and R. P. J., “Between classical and quantum monte carlo methods: variational qmc,” in *Advances in Chemical Physics: Monte Carlo Methods in Chemical Physics* (I. Prigogine and S. A. Rice, eds.), vol. 105, John Wiley and Sons, Inc.
- [24] P. Ewald, “Die berechnung optischer und elektrostatischer gitterpotentiale,” *J. Chem. Phys.*, vol. 369, pp. 253–287, 1921.
- [25] V. Natoli and D. Ceperley, “An optimized method for treating long-range potentials,” *Journal of Computational Physics*, vol. 117, pp. 171 – 178, 1995.
- [26] G. Giuliani and G. Vignale, *Quantum Theory of the Electron Liquid*. Cambridge, UK: Cambridge University Press, 2005.
- [27] D. Ceperley, G. Chester, and M. Kalos, “Monte carlo simulation of a many-fermion study’,” *Phys. Rev. B*, vol. 16, no. 7, pp. 3081–3099, 1977.
- [28] F. Rapisarda and G. Senatore, “Diffusion monte carlo study of electrons in two-dimensional layers,” *Aust. J. Phys.*, vol. 49, pp. 161–182, 1996.
- [29] R. Feynman and A. Hibbs, *Quantum Mechanics and Path Integrals*. New York, USA: McGraw-Hill, 1965.
- [30] G. Box and M. Müller, “A note on the generation of random normal deviates,” *Ann. Math. Statist.*, vol. 29, no. 2, pp. 610–611, 1958.